

Competition of fusion and quasi-fission in the reactions leading to production of the superheavy elements

M. Veselsky*

Institute of Physics, Slovak Academy of Sciences, Bratislava, Slovakia

The mechanism of fusion hindrance, an effect observed in the reactions of cold, warm and hot fusion leading to production of the superheavy elements, is investigated. A systematics of trans-fermium production cross sections is used to determine fusion probabilities. Mechanism of fusion hindrance is described as a competition of fusion and quasi-fission. Available evaporation residue cross sections in the superheavy region are reproduced satisfactorily. Analysis of the measured capture cross sections is performed and a sudden disappearance of the capture cross sections is observed at low fusion probabilities. A dependence of the fusion hindrance on the asymmetry of the projectile-target system is investigated using the available data. The most promising pathways for further experiments are suggested.

Introduction

In the recent years, the heavy elements up to $Z=112$ have been synthesized using cold fusion reactions with Pb, Bi targets in the evaporation channel with emission of one neutron [1]. The experimentalists had to face a steep decrease of cross sections up to the picobarn level due to increasing fusion hindrance whose origin was unclear. The same level of cross sections has been reached in the hot fusion reactions with emission of 3-4 neutrons using ^{48}Ca beams which lead to synthesis of relatively neutron-rich isotopes of elements 112,114 and 116 [2, 3, 4, 5]. Again the fusion hindrance was observed. The possibility to describe fusion hindrance in both cold and hot fusion in a unified way as a competition between formation of the compound nucleus and a fast fission-like process (quasi-fission) was suggested in our article [6] using a simple phenomenological model. A comparison of the recent experimental results to the results of the model calculation is provided in the present article. Furthermore, additional investigations on the nature of the fusion process are carried out using available data on capture cross section. An additional dynamical fusion hindrance is predicted based on available experimental evaporation residue data from the reactions where heavy nuclei are produced in the symmetric projectile-target combinations approaching the asymmetry of the fission channel.

Statistical model for competition of fusion and quasi-fission

In our previous article [6], we presented a simple statistical model for the description of production cross sections of superheavy nuclei in a wide range of excitation energies including cold, warm and hot fusion. The model assumes that the fusion hindrance, observed in cold fusion reactions where only one neutron is emitted prior to the formation of evaporation residue (ER), can be explained by the competition of fusion with fast fission-like process which can be identified with quasi-fission. It is not obvious what is the role of a traditional saddle configuration, used in description of fusion-fission, in quasi-fission. Therefore, the scission configuration was chosen as a final state in the fission channel. Then the fusion probability can be expressed using the level densities in compound and scission configurations as

$$P_{\text{fus}}^{\text{stat}} = \frac{\rho(E_{\text{CN}}^*)}{\rho(E_{\text{CN}}^*) + \rho(E_{\text{sc,eff}}^*)}. \quad (1)$$

The excitation energy in the scission configuration is estimated empirically using the systematics of post-scission neutron multiplicities. Proportionality of the number of neutrons emitted from the fission fragments to the intrinsic excitation energy in the scission configuration is assumed. Then the excitation energy in the scission configuration can be expressed as

*Electronic address: fyzimarv@savba.sk

$$E_{\text{sc,eff}}^* = (\nu_n^{\text{s.f.}}(A_{\text{CN}}) + \Delta\nu_n(E_{\text{CN}}^*))E_n. \quad (2)$$

The multiplicity of emitted neutrons in the spontaneous fission of heavy nuclei $\nu_n^{\text{s.f.}}(A_{\text{CN}})$ is approximated by a linear extrapolation of the available spontaneous fission neutron multiplicity data to given A_{CN}

$$\nu_n^{\text{s.f.}}(A_{\text{CN}}) = 3.316 + 0.0969(A_{\text{CN}} - 250). \quad (3)$$

An additional increase of the post-scission neutron multiplicity at a given excitation energy $\Delta\nu_n(E_{\text{CN}}^*)$ can be expressed approximately as

$$\Delta\nu_n(E_{\text{CN}}^*) = 0.035E_{\text{CN}}^*, \quad (4)$$

as follows from the available post-scission neutron multiplicity data [7]. A proportionality factor E_n is the amount of intrinsic excitation energy per emitted neutron. This is a free parameter and it was estimated from the systematics of production cross sections of transfermium nuclei produced in cold and hot fusion.

The unhindered fusion cross sections have been calculated using one-dimensional WKB approximation with Gaussian barrier width distribution [8] implemented into the statistical code HIVAP [9]. Such an approximation proved quite successful despite its simplicity. The depth of the nuclear potential well is taken as $V_0=40$ MeV, the half-density radius as $r_0=1.11$ fm and the diffuseness is set to $d=0.75$ fm. The width of barrier distribution ranges from 3 % for reactions with the doubly magic nucleus ^{208}Pb to 5 % for reactions with heavy deformed nuclei away from the shell closure.

The survival probabilities were calculated using a conventional statistical calculation. The competition of fission vs particle emission was calculated using a modified version of HIVAP code [9] with fission barriers expressed as [10]

$$B_f(l) = C(B_f^{\text{LD}}(l) + \Delta B_f^{\text{Shell}}). \quad (5)$$

The liquid drop component of the fission barrier (B_f^{LD}) has been calculated according to the rotating charged liquid drop model of Cohen-Plasil-Swiatecki [11]. The shell component of the fission barrier ($\Delta B_f^{\text{Shell}}$) has been approximated by a value of the ground state shell correction taken from the calculation of Moller [12]. Such an approximation for the fission barriers proved successful for description of the evaporation residue cross sections in the region around neutron shell closure $N=126$ where the value of the parameter C proved to be practically constant for the large set of evaporation residues with the values of the ground state shell correction ranging from zero up to 8 MeV [10].

The shell corrections for transfermium nuclei are expected to be within the same range while the liquid drop fission barriers are virtually zero. The optimum values of parameter C , necessary to reproduce experimental cross sections of the evaporation residues with $Z>100$, are given in Figure 1 as a function of atomic number. One can see that the optimum values of C for the hot fusion reactions remain stable within $Z = 102 - 110$. The value of $C = 0.8 - 0.9$ is higher when compared to $N=126$ region and this difference could be most probably attributed to differences of saddle point configurations in both regions.

Unlike for the hot fusion products, the optimum values of the parameter C for the cold fusion reactions with ^{208}Pb target are increasingly falling out of systematics at $Z > 104$ what can be attributed to emerging competition of the fusion with quasi-fission. Thus, the fusion probabilities for cold fusion were obtained by comparing the measured evaporation residue cross sections with those calculated using C from the hot fusion systematics. The parametrization $E_n = 3.795 + 0.04(A_{\text{CN}} - 260)$ for the parameter in the formula 2 was obtained and used in further calculation for nuclei with $Z>110$.

The alternative scenario of the fusion hindrance originating from tunneling through the barrier in the sub-barrier region seems to be contradiction with experimental ratios of the cross sections in 1n and 2n evaporation channels of reactions with ^{208}Pb target [1] which increase from about 0.1 for ^{48}Ca -beam ($Z=102$) to 10 for ^{58}Fe -beam ($Z=108$). Such a situation suggests that even at excitation energies corresponding to 1n channel the reaction can not be considered of a sub-barrier type.

Table 1 gives the production cross sections of several new superheavy nuclei [2, 3, 4, 5], reported since our initial article [6] was published, compared to the maximum evaporation residue cross sections in xn channels estimated in [6]. No angular momentum dependence for description of the scission point was assumed and the cross sections were

evaluated in the maxima of the excitation functions obtained from statistical calculations with no fusion hindrance assumed. One can see that the calculation predicted production cross sections rather well for the reaction $^{48}\text{Ca}+^{238}\text{U}$. For heavier systems the estimated cross sections are lower by up to one order of magnitude since calculation exhibits systematic shift in the dominating xn evaporation residue channel toward higher number of emitted neutrons. The discrepancy observed can be attributed to the simplification used in the initial calculation where the unhindered maximum production cross sections obtained using HIVAP code were multiplied by the fusion probabilities with no angular momentum dependence assumed. Recently, the calculation was corrected [13] by implementing an angular momentum into the description of the compound nucleus and scission configuration and by introducing the fusion probability calculation for each partial wave into HIVAP code. The moment of inertia of symmetric touching rigid spheres was used for the scission configuration. An improved version of HIVAP code uses the fusion probability for each partial wave as a multiplication factor to the unhindered fusion cross section. This allows to obtain more realistic shapes of excitation functions for evaporation residue channels.

In Table 2 are again given production cross sections of the recently synthesized superheavy nuclei, compared to the results of improved calculation [13]. The production cross sections track quite well with the reported ones. New calculation reproduces reasonably well not only the absolute values but also the positions of the maxima and thus promises possibility for further estimates. Concerning the recently reported [14] (and more recently corrected [15]) experimental results from the reaction $^{86}\text{Kr}+^{208}\text{Pb}$, the calculation (as published in [13]) lead to estimated production cross section for 1n channel of approximately 10^{-4} pb. Such a value was in contradiction with initial experimental cross section value 2.2 pb [14] but it is consistent with the corrected experimental results. As stated above, the parametrization of E_n used was obtained using data from cold fusion only and thus the estimated cross section for cold fusion is practically just an extrapolation of cross section trend. In any case, significant success of the extrapolation when used for hot fusion reactions virtually justifies its validity also for cold fusion reactions. Therefore, the cold fusion reactions do not seem to offer much promise for further progress in the synthesis of superheavy nuclei.

In Table 3 are given predictions for several reactions which may lead to the synthesis of even heavier nuclei. An improved calculation [13] was used in this case. Only reactions of stable beams with stable or long-lived targets have been taken into account. The reactions $^{48}\text{Ca}+^{249}\text{Cf}$ and $^{58}\text{Fe}+^{238}\text{U}$ give promise for the synthesis of the isotope $^{292,293}118$ on the cross section level of 0.1-0.2 pb which seems to be an experimental limit for the foreseeable future. Compared to the system $^{58}\text{Fe}+^{238}\text{U}$, the choice of heavier projectile ^{64}Ni or target ^{244}Pu leads to the drop of cross section by one and half orders of magnitude. It is necessary to note that the quality of the estimate directly depends on the prediction of the masses and ground state shell corrections [12] used in the calculation. The results given in Table 2 suggest that the masses and ground state shell corrections used are quite realistic. Nevertheless, any discrepancies in further extrapolation will affect the cross section estimates significantly.

Capture cross sections

In order to understand the competition of the fusion and quasi-fission it is of great interest to investigate also the measured cross sections of the fusion-fission and quasi-fission. Such an analysis was performed on the data on measured capture cross sections [16] (defined in the experiment as the cross section of the fission events with the total kinetic energy and fragment masses outside of the quasi-elastic/deep-inelastic region of the TKE vs mass matrix). The experimental setup used was optimized to detect fusion-fission for each specific reactions. A comparison of the experimentally determined capture cross sections [16] to the calculated unhindered fusion cross sections [8] and fusion probabilities [6, 13] is presented in Figures 2,3. As one can see from the Fig. 2 the calculated fusion cross sections track very well with the measured capture cross sections for the reactions $^{48}\text{Ca}+^{208}\text{Pb}$ and $^{58}\text{Ca}+^{208}\text{Pb}$. For the heavier systems the measured capture cross sections become smaller than the calculated fusion cross sections. Such an effect appears to increase with decrease of the excitation energy of the compound nucleus. One can assume that such a discrepancy can be related to decrease of the fusion probability for the heavier systems. Such an assumption is examined in the Fig. 3 where the ratio of the measured capture cross section to the calculated unhindered fusion cross sections is represented as a function of the fusion probability calculated as in [13]. One can observe a surprising abrupt disappearance of the measured capture cross section at fusion probabilities below 10^{-6} . Such an abrupt disappearance of the measured capture cross section when compared to the calculated fusion cross section seems to be rather global and it may indicate a dramatic change of the properties of reaction products due to different dynamical evolution. A possibility to explain the trend qualitatively is presented in Figure 4 in the framework of "toy model" mimicking a competition of multi-step dynamical evolution toward fusion with a possibility of irreversible exit into the quasi-fission channel at each step. Fusion probability is treated as a product of N elementary sub-probabilities $P(i)$ corresponding to elementary steps of the evolution toward fusion. The probability for the first step $P(1)$ is assumed one, later the

probability decreases linearly until it reaches minimum halfway toward fusion, then the probability starts to increase linearly and the probability of the last step is again assumed one. At each step, the quantity $1-P(i)$ can be considered the probability of exit into quasi-fission channel. The resulting exit channel probability density of fusion-quasi-fission competition with 100 steps is superimposed onto the exit channel probability density of another process with the exit channel probability density quickly exponentially decreasing with step number. The latter process is considered 10 times more frequent. Such a procedure can simulate an interplay with the quasi-elastic/deep-inelastic reactions occurring at the partial waves close to the grazing angular momentum (and thus with higher cross section). As one can see with decreasing fusion probability the exit channel probability densities of two processes increasingly overlap and at some point can not be decomposed anymore. This can be a qualitative explanation for the situation in Fig. 3 where the measured capture cross-section initially tracks with the calculated fusion cross section but at some point this correspondence disrupts abruptly. In the realistic process leading to either fusion or quasi-fission, the concentration of the probability density at the early stage of dynamical evolution may lead to kinematic properties of the fission fragments very different from the fusion-fission. Such a fragments can become undetectable using a given experimental setup optimized for detection of the fusion-fission products. In any case the disappearance of the measured capture cross sections in a given case can be understood as a signature of the interconnection of the fusion and the quasi-fission processes within the concept of their competition during the multi-step dynamical evolution of the system.

Symmetric systems

Of great interest for the future prospects of synthesis of superheavy nuclei is the understanding of reaction dynamics in the case where both projectile and target are of comparable size. In order to investigate a possible fusion hindrance originating from increasing symmetry of the projectile-target system we compared the calculated evaporation residue cross section in the four reactions leading to compound nucleus ^{246}Fm to the experimental cross sections from the work of Gaeggeler et al. [17]. The calculation used was identical to [13]. The result is presented in the Table 4. When looking at the results and taking into account the systematics in Fig. 1 where fusion hindrance occurs for cold fusion of compound nuclei with $Z > 104$, one can assume that there appear to exist additional fusion hindrances which emerge with increasing symmetry of the reaction.

In order to understand a possible nature of such hindrances we carried out an analysis of the data in the Pb-U region [18, 19]. Using the fusion model with WKB and Gaussian barrier distribution [8] and fission channel parameters from the systematics for given region [10] ($C \approx 0.65$) we observe an interesting behavior (see Fig. 5). For the reaction $^{100}\text{Mo} + ^{100}\text{Mo}$ the evaporation residue cross section is described well. In the transition to $^{110}\text{Pd} + ^{110}\text{Pd}$ there is an increasing hindrance at low excitation energies. The hindrance factor seems to increase with decreasing excitation energy. To some surprise, the same effect can be seen also in the transition from $^{100}\text{Mo} + ^{100}\text{Mo}$ to $^{100}\text{Mo} + ^{92}\text{Mo}$ (lighter system but with higher fissility). Also of interest is the fact that experimental cross section data for Pd+Ru and Pd+Pd systems are only in the region above calculated fusion barrier where calculated fusion cross remain stable but disappear in the sub-barrier region where calculated cross sections start to drop quickly.

In order to test the fusion cross section model, the measured and calculated xn evaporation cross section for four systems leading to compound nucleus ^{220}Th ($^{40}\text{Ar} + ^{180}\text{Hf}$ [20], $^{124}\text{Sn} + ^{96}\text{Zr}$ [21], $^{48}\text{Ca} + ^{172}\text{Yt}$ and $^{70}\text{Zn} + ^{150}\text{Gd}$ [22]) are given in the Fig. 6. The calculations have been performed using HIVAP code. The barrier distribution widths [8] used comply to the usual prescription (5 % for Ar+Hf, Ca+Yt and Zn+Gd since (heavy) target is deformed and 4 % for Sn+Zr since (heavier) projectile is close to spherical). The shapes of xn excitation functions are reproduced reasonably well, especially the ascending/barrier part and the maximum of xn excitation functions are reproduced acceptably. The fission barrier scaling parameter C [10] was equal for Ar+Hf and Ca+Yt ($C=0.67$) and Zn+Gd and Sn+Zr ($C=0.61$). The discrepancy in C is not fully compliant with the concept of compound nucleus, since it should be the same in all cases. Most probably it is caused by the irregularities in alpha-emission where especially in the symmetric systems the memory of the entrance channel (e.g. deformation) may lead to enhanced emission of the alpha-particles and thus to reduction of xn cross sections. Experimental alpha-particle emission spectra [23] suggest alpha emission barriers of about 90 % of the alpha-particle fusion barrier what is also used in calculations but such a prescription is rather simplistic and may not account for dynamical effects in symmetric reactions. Apart from entrance channel memory, an admixture from incomplete fusion channels with emission of alpha-particle is also possible. More detailed data will be necessary for complete understanding of the phenomena. In any case, the description of the fusion barrier by the approximation employed can be considered adequate.

Further comparisons of the calculated and experimental evaporation residue cross sections for reactions leading to various Th compound nuclei are given in Fig. 7. The maximum cross sections for various xn evaporation channels are

considered. For the compound system ^{214}Th where one can see a strong hindrance for reaction $^{110}\text{Pd}+^{104}\text{Ru}$ (see Fig. 5) the same can not be concluded for the reaction $^{124}\text{Sn}+^{90}\text{Zr}$ [24]. Also, for Th compound nuclei ranging from ^{214}Th to ^{222}Th no hindrance can be observed for reactions including $^{32}\text{S}+^{182}\text{W}$ [25], $^{60}\text{Ni}+^{154}\text{Sm}$ [25], $^{64}\text{Ni}+^{154}\text{Sm}$ [26] and $^{86}\text{Kr}+^{136}\text{Xe}$ [27]. For $^{86}\text{Kr}+^{136}\text{Xe}$ data the xn cross sections are practically constant from 1n to 6n channel what is in conflict with extra-push theory [28]. As in the previous case the fission barrier scaling parameter C varied from 0.6 to 0.67 and emission barriers were 10 % lower than fusion barriers for a given light charged particle. The widths of the fusion barrier distribution were consistent to above prescription. As one can see from Figs. 6 and 7, statistical model calculation with fission barriers compliant to the formula 5 (giving equally good description for nuclei with and without strong g.s. shell corrections [10]) and with fusion cross section calculated using one-dimensional WKB approximation with fusion barrier distribution provides very consistent description of the evaporation residue cross sections virtually without using free parameters. No fusion hindrance can be observed for a wide range of compound nuclei. Thus one can conclude that the fusion hindrance in Th-region takes place only for the reactions leading to highly fissile compound nuclei with projectile-target asymmetry in narrow region close to zero.

When looking for an explanation of the above behavior one can turn attention to the properties of the fission fragments in the given region. Recent studies of low energy fission in Ac-U region [29, 30] show that there is a systematic transition from asymmetric to symmetric fission around the mass 222-226. The Th compound nuclei studied above all fall into the region with symmetric fission mode. Thus, one can assume that an additional fission hindrance appears when the asymmetry of fusion channel is close to the asymmetry of fission channel. There, one can assume that immediate fission is highly favored dynamically over the long evolution toward fusion. For the heavier nuclei with masses above 226 the dominant fission mode at low excitation energies is the mode where one fragment (heavier one for lighter nuclei and lighter one for very heavy nuclei) is of the mass approximately 132 and the mass of the other fragment increases linearly with the mass of fissioning system [16]. The reaction $^{136}\text{Xe}+^{110}\text{Pd}$ studied by Gaeggeler et al. [17] is virtually an inverse fission and a dynamical fusion hindrance can be understood there. The reactions $^{76}\text{Ge}+^{170}\text{Kr}$, $^{86}\text{Kr}+^{160}\text{Gd}$ are far away from the main fission mode but still match the super-asymmetric mode (with the maximum yields of light fragment positioned around ^{82}Ge) which is usually necessary to reproduce the experimental mass distributions [31]. Thus, the knowledge of fission modes in transfermium region seems to be an essential information for the study of fusion probability. An interesting test for such an assumption would be a reaction $^{132}\text{Sn}+^{96}\text{Zr}$ leading to compound nucleus ^{228}Th which fissions asymmetrically and thus it would be an inverse fission again and hindrance factors should appear. The non-hindered cross sections can be expected in mb region so already a relatively moderate beam of ^{132}Sn may be sufficient to show discrepancy. The use of radioactive beam is essential in this case since no symmetric combination of the stable beam and target appears to reach Th isotopes beyond 222.

Summary and conclusions

In summary, the possibilities for synthesis of new superheavy elements using stable or long-lived projectiles and targets seem to be rather restricted. The parametrization of model parameters able to reproduce existing experimental results predicts a possibility to synthesize isotopes of element 118 in hot fusion reactions at the cross section level 0.1 pb. Concerning the nature of the process, the analysis of the measured cross sections suggests that the competition of fusion and quasi-fission is a multi-step dynamical process and that the low fusion probability is consistent with the fast re-separation of the reacting system even at low partial waves. For symmetric systems where the asymmetry of the projectile-target combination approaches the asymmetry of the fission channel an additional fusion hindrance caused by dynamical dominance of immediate re-separation into the fission channel over long evolution toward complete fusion seems to take place. Such a dynamical hindrance can strongly reduce the possible pathways toward superheavy elements. A knowledge on fission fragment asymmetry seems to be essential for further studies of synthesis of superheavy elements.

The author would like to thank S. Hofmann, A.V. Yeremin, J. Peter, R. Smolanczuk, G. Chubarian, E.M. Kozulin, W. Loveland and G.A. Souliotis for fruitful discussions. Furthermore, the author would like to thank Yu.Ts. Oganessian and M.G. Itkis for their interest to this work. This work was supported through grant VEGA-2/1132/21.

[1] S. Hofmann, Rep. Prog. Phys. **61**, 639 (1998).

[2] A.V. Yeremin et al., Eur. Phys. J. A **5**, 63 (1999).

- [3] Yu.Ts. Oganessian et al., *Nature*, **400**, 242 (1999).
- [4] Yu.Ts. Oganessian et al., *Phys. Rev. C* **62**, 41604 (2000).
- [5] Yu.Ts. Oganessian et al., *Phys. Rev. C* **63**, 11301 (2000).
- [6] M. Veselsky, *Acta Phys. Slovaca* **49**, 101 (1999).
- [7] S.M. Lukyanov et al., *Proc. Int. School of Heavy Ion Phys.*, Dubna, 3-12 Oct 1989, JINR Dubna, 1990, p.225; D. Hilscher et al., *Phys. of Atom. Nucl.* **57**, 1187 (1994).
- [8] W. Reisdorf et al., *Nucl. Phys. A* **444**, 154 (1985).
- [9] W. Reisdorf, *Z. Phys. A* **300**, 227 (1981).
- [10] M. Veselsky, PhD Thesis, Comenius University, Bratislava, 1997; see also D.D. Bogdanov et al., *Phys. of Atom. Nucl.*, **62**, 1794 (1999).
- [11] S. Cohen, F. Plasil, W.J. Swiatecki, *Ann. Phys. (N.Y.)* **82**, 557 (1974).
- [12] P. Moller et al, *Atomic Data and Nuclear Data Tables* **59**, 185 (1995).
- [13] M. Veselsky, *Progress in Research, 2000–2001*, Cyclotron Institute, Texas A&M University, p. II-30; see also http://cyclotron.tamu.edu/progress/2000-2001/2_a12.pdf.
- [14] V. Ninov et al., *Phys. Rev. Lett.* **83**, 1104 (1999).
- [15] K.E. Gregorich et al., *nucl-ex/0201014*.
- [16] M.G. Itkis et al., *Proc. of Int. Workshop on Fusion Dynamics at Extremes*, Dubna, Russia, 25-27 May 2000, World Scientific, Singapore, 2001, p. 93.
- [17] H.W. Gäggeler et al., *Z. Phys. A* **316**, 291 (1984).
- [18] W. Morawek et al., *Z. Phys. A* **341**, 75 (1991).
- [19] A.B. Quint et al, *Z. Phys. A* **346**, 119 (1993).
- [20] D. Vermeulen et al., *Z. Phys. A* **318**, 157 (1984).
- [21] C.C. Sahm et al., *Z. Phys. A* **319**, 113 (1984).
- [22] J. Peter et al., *Proc. of Int. Conf. Nuclear Physics at Border Lines*, Lipari, Italy, 21-24 May 2001, World Scientific, Singapore, 2002, p. 257.
- [23] L.C. Vaz and J.M. Alexander, *Z. Phys. A* **318**, 231 (1984).
- [24] C.C. Sahm et al., *Nucl. Phys. A* **441**, 316 (1985).
- [25] S. Mitsuoka et al., *Phys. Rev. C* **62**, 54603 (2000).
- [26] S. Mitsuoka et al., *Phys. Rev. C* **65**, 54608 (2002).
- [27] R.N. Sagaidak et al., *Proc. of VI Int. School-Seminar on Heavy Ion Physics*, Dubna, Russia, 22-27 Sept 1997, World Scientific, Singapore, 1998, p. 323.
- [28] J. Blocki, H. Feldmeier and W. Swiatecki, *Nucl. Phys. A* **459**, 145 (1986).
- [29] K.-H. Schmidt et al., *Nucl. Phys. A* **665**, 221 (2000).
- [30] I.V. Pokrovsky et al., *Phys. Rev. C* **62**, 14615 (2000).
- [31] V.A. Rubchenya and J. Äystö, *Nucl. Phys. A* **701**, 127c (2002).

TABLE I: Comparison of several recently reported production cross sections of elements with $Z > 110$ [2, 3, 4, 5] to the predictions published in [6].

Reaction	Experiment		Calculation	
	ER	σ_{ER}	ER	σ_{ER}
$^{48}\text{Ca} + ^{238}\text{U}$	$^{283}_{112}$	5 pb	$^{283}_{112}$	1.5 pb
$^{48}\text{Ca} + ^{242}\text{Pu}$	$^{287}_{114}$	2.5 pb	$^{286}_{114}$	0.25 pb
$^{48}\text{Ca} + ^{244}\text{Pu}$	$^{288}_{114}$	0.7 pb	$^{287}_{114}$	0.1 pb
$^{48}\text{Ca} + ^{248}\text{Cm}$	$^{292}_{116}$	0.3 pb	$^{291}_{116}$	0.01 pb

TABLE II: Comparison of recently reported production cross sections of elements with $Z > 110$ [2, 3, 4, 5] to the results of the improved calculations [13].

Reaction	E_{lab} [MeV]	ER	σ_{ER} [pb]	
			Exp.	Calc.
$^{48}\text{Ca} + ^{238}\text{U}$	231	$^{283}_{112}$	5	4
$^{48}\text{Ca} + ^{238}\text{U}$	238	$^{282}_{112}$	≤ 7	8
$^{48}\text{Ca} + ^{242}\text{Pu}$	235	$^{287}_{114}$	2.5	1.5
$^{48}\text{Ca} + ^{244}\text{Pu}$	236	$^{288}_{114}$	0.7	2.0
$^{48}\text{Ca} + ^{248}\text{Cm}$	240	$^{292}_{116}$	0.3	0.1

TABLE III: Predictions of production cross sections of elements with $Z > 116$ calculated using improved calculation [13]. Reactions of stable beams with stable or long-lived targets have been taken into account.

Reaction	E^* , MeV	ER	$\sigma_{ER}(\text{calc})$
$^{48}\text{Ca} + ^{249}\text{Cf}$	47	$^{293}_{118}$	0.1 pb
$^{48}\text{Ca} + ^{249}\text{Cf}$	52	$^{292}_{118}$	0.25 pb
$^{48}\text{Ca} + ^{252}\text{Cf}$	46	$^{296}_{118}$	0.02 pb
$^{48}\text{Ca} + ^{252}\text{Cf}$	53	$^{295}_{118}$	0.03 pb
$^{58}\text{Fe} + ^{238}\text{U}$	48	$^{292}_{118}$	0.2 pb
$^{58}\text{Fe} + ^{244}\text{Pu}$	56	$^{297}_{120}$	0.007 pb
$^{64}\text{Ni} + ^{238}\text{U}$	56	$^{297}_{120}$	0.007 pb

TABLE IV: Comparison of the calculated evaporation residue cross section in the four reactions leading to compound nucleus ^{246}Fm to the experimental cross sections from the work of Gaeggeler et al. [17].

Reaction	$\sigma_{2n}(\text{exp})$	$\sigma_{2n}(\text{calc})$
$^{40}\text{Ar} + ^{206}\text{Pb}$	3 nb	1 nb
$^{76}\text{Ge} + ^{170}\text{Er}$	1 nb	19 nb
$^{86}\text{Kr} + ^{160}\text{Gd}$	< 0.3 nb	26 nb
$^{136}\text{Xe} + ^{110}\text{Pd}$	< 0.2 nb	40 nb

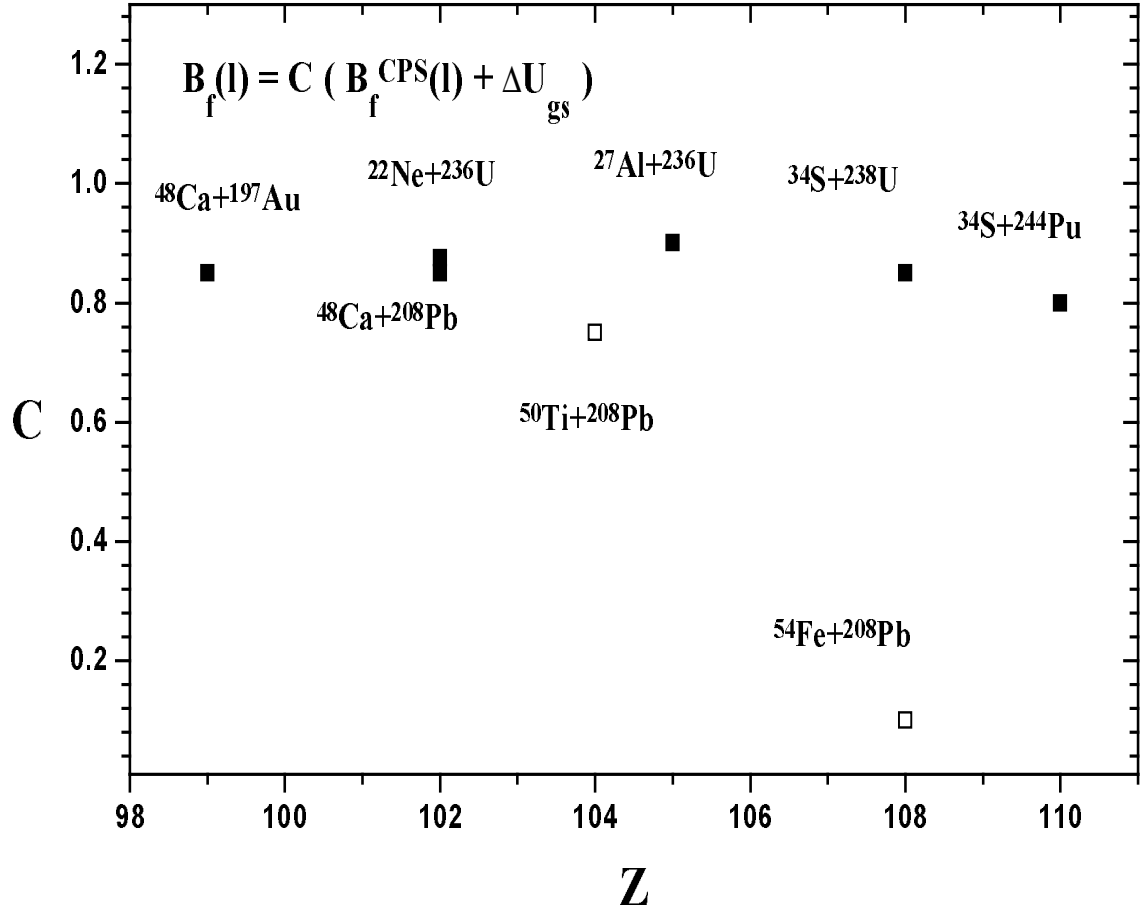


FIG. 1: Optimum values of parameter C , necessary to reproduce experimental cross sections of hot fusion reactions (solid symbols), as a function of atomic number of residual nuclei. Open symbols - cold fusion reactions.

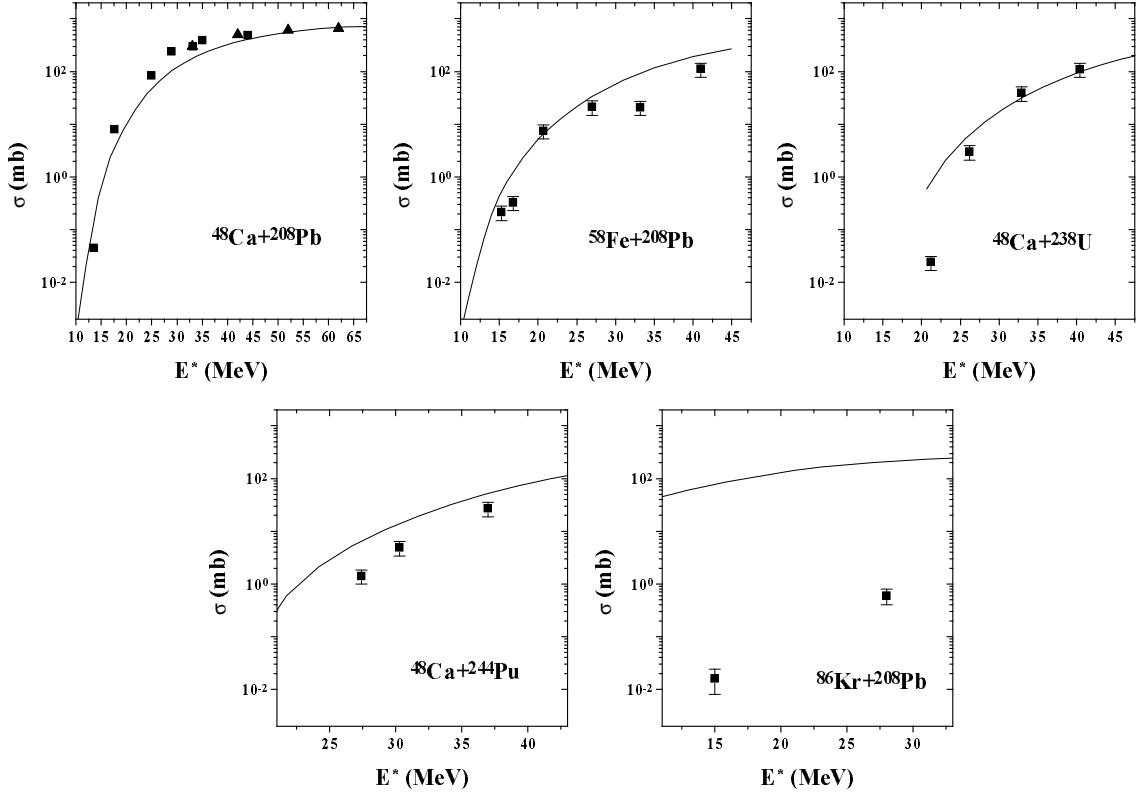


FIG. 2: Experimental capture cross sections [16] (symbols) and the fusion cross sections calculated using WKB approximation with Gaussian barrier distribution [8] (lines). Data from five different reactions are presented. Width of barrier distribution is assumed 3% for ^{208}Pb target and 5% for ^{238}U and ^{244}Pu targets.

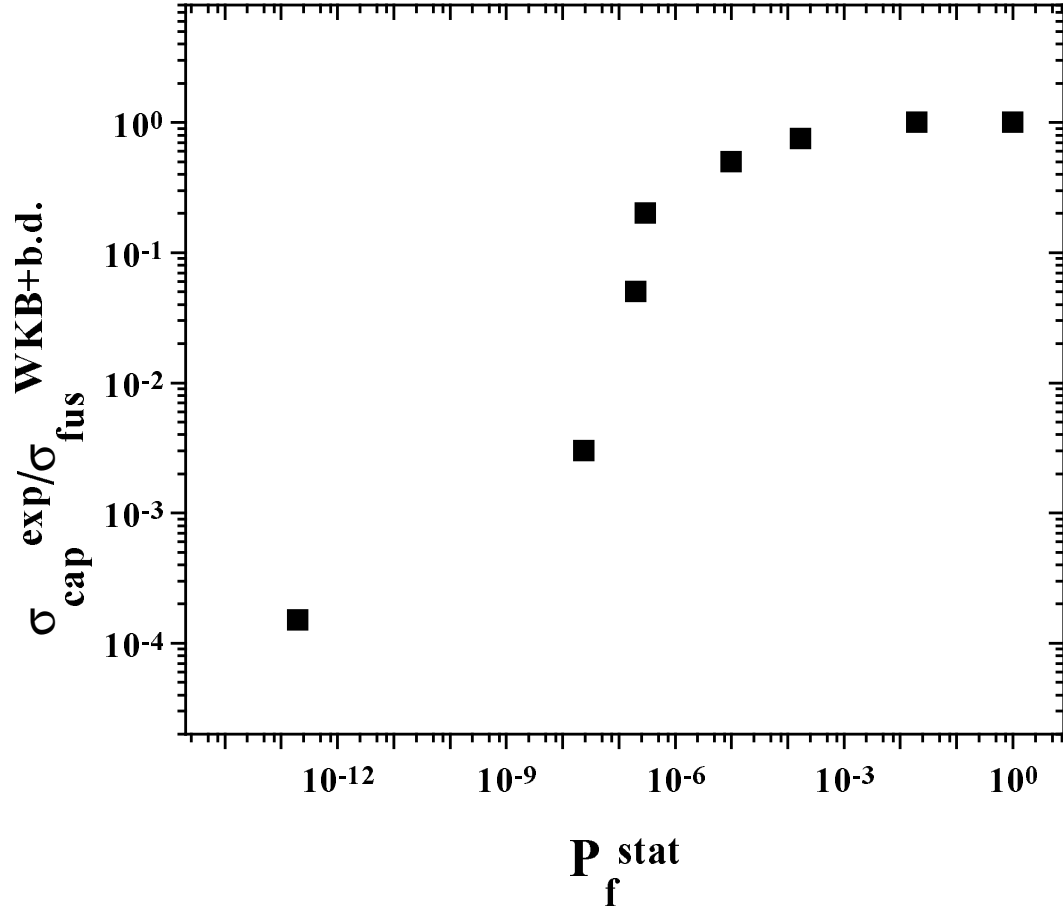


FIG. 3: Ratio of the experimental capture cross sections [16] to the fusion cross sections calculated using WKB approximation with Gaussian barrier distribution [8] (symbols) plotted as a function of the calculated fusion probability [6, 13]. The data points from Fig. 2 are used.

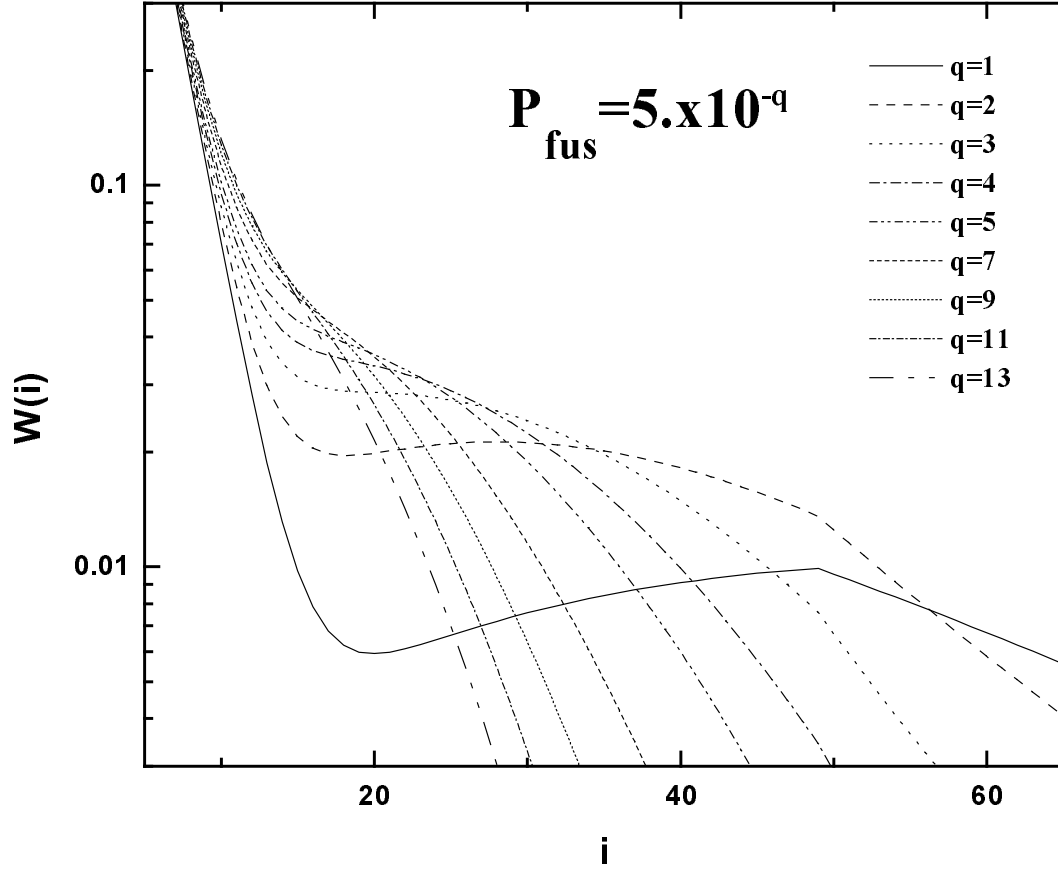


FIG. 4: "Toy model" description of the fusion-fission vs quasi-fission competition during the dynamical evolution of the system. The exit channel probability density $W(i)$ is plotted as a function of step number i for several values of the resulting fusion probability P_{fus} . For details see text.

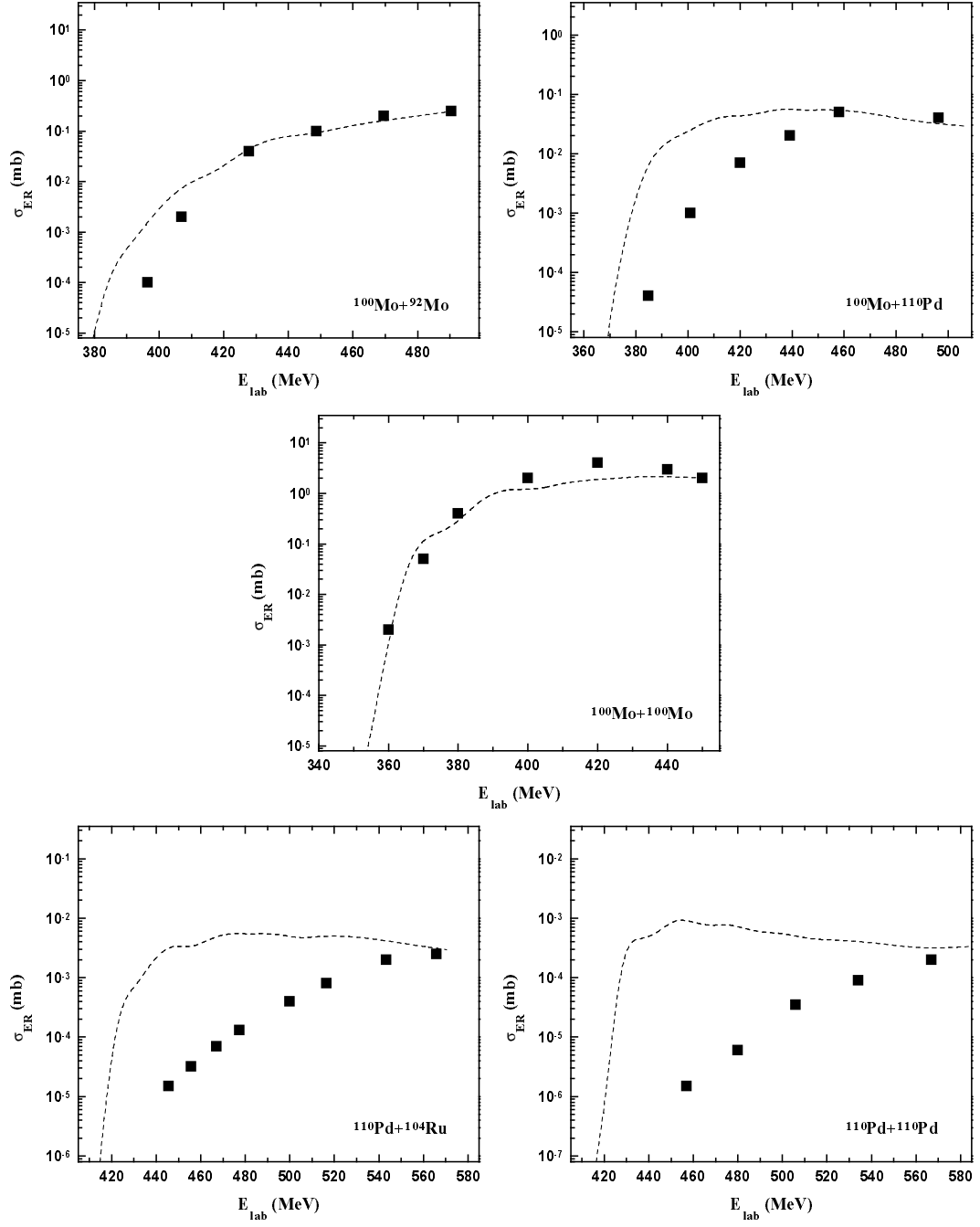


FIG. 5: Comparison of the measured [18, 19] and calculated evaporation residue cross sections for several symmetric systems.

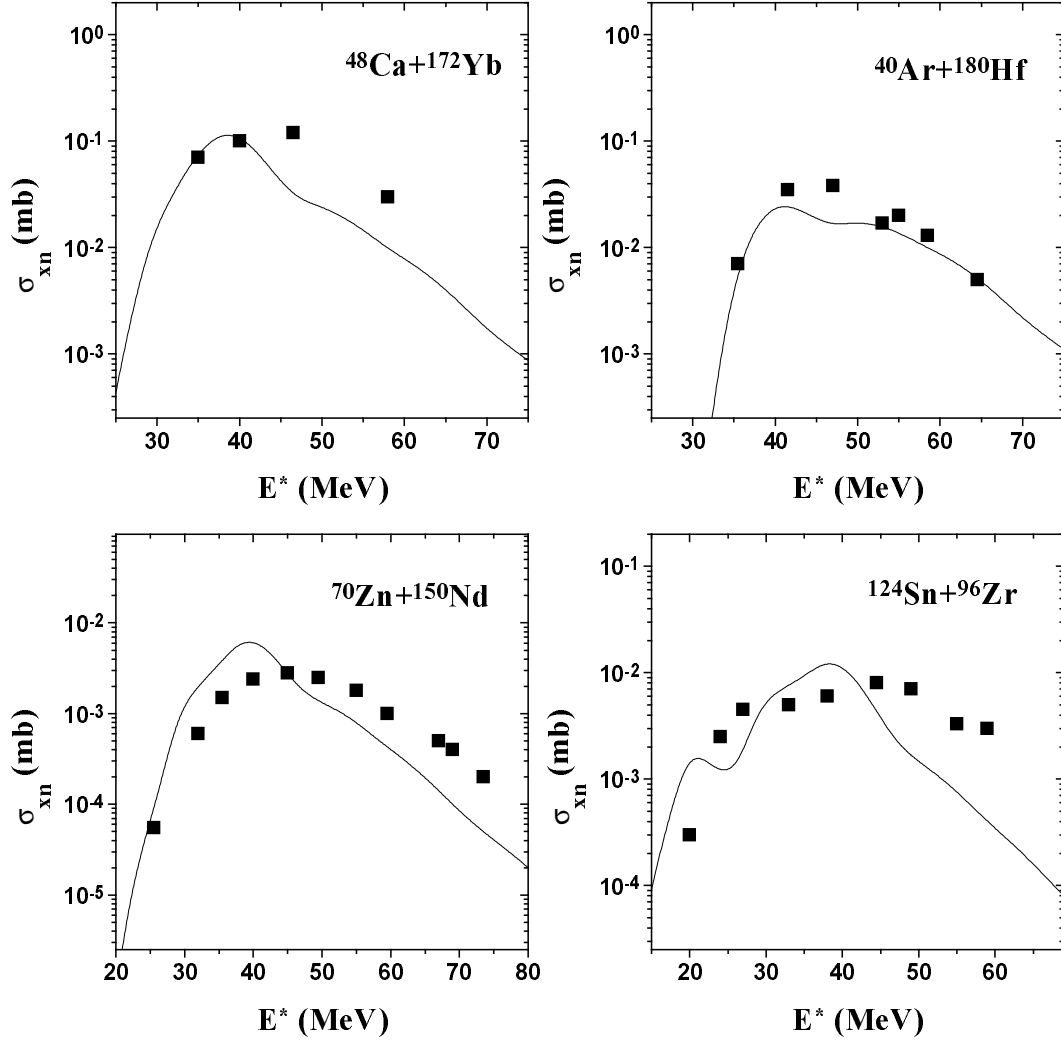


FIG. 6: Comparison of the measured [20, 21, 22] and calculated xn evaporation residue cross sections for several systems leading to the compound nucleus ^{220}Th .

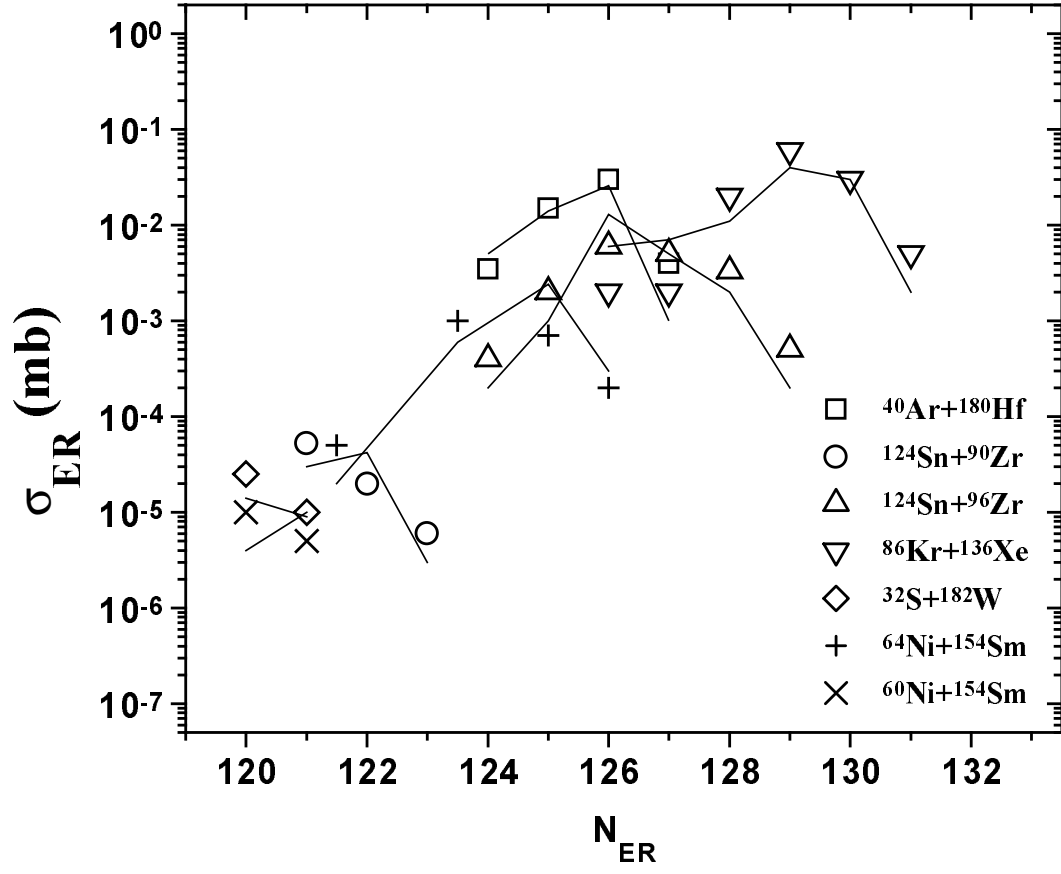


FIG. 7: Comparison of the measured [20, 21, 24, 25, 26, 27] and calculated maximum xn evaporation residue cross sections for several systems leading to various Th compound nuclei.